Influence of the Polydispersity of Polymeric Surfactants on the Enantioselectivity of Chiral Compounds in Micellar Electrokinetic Chromatography

Jepkoech Tarus,[†] Rezik A. Agbaria,[†] Kevin Morris,[‡] Simon Mwongela,[†] Abdulqawi Numan,[†] Lindah Simuli,[†] Kristin A. Fletcher,[†] and Isiah M. Warner*,[†]

Department of Chemistry, Louisiana State University, Baton Rouge, Louisiana 70803, and Department of Chemistry, Carthage College, Kenosha, Wisconsin 53140

Received December 12, 2003. In Final Form: May 14, 2004

Poly(sodium undecenoyl-L-leucinate) (poly-L-SUL) was fractionated by the use of different molecular weight cutoff (MWCO) filters to narrow the polydispersity of the macromolecular sizes of the polymeric surfactant. The resulting polymeric surfactant fractions were characterized by the use of three techniques: (1) pulsed field gradient nuclear magnetic resonance (PFG-NMR) was used to determine the hydrodynamic radii, (2) analytical ultracentrifugation (AUC) was used to determine the molecular weights, and (3) steady-state fluorescence was used to determine the polarity of the nonfractionated and fractionated polymeric surfactants. From the data acquired from PFG-NMR, AUC, and fluorescence, it was noted that the hydrodynamic radii and molecular weight of the fractionated poly-L-SUL increased, while the polarity decreased with the increase in the size of the MWCO filter. However, a similarity in physical properties was observed between the nonfractionated and 10−30K fractionated poly-L-SUL except for the hydrodynamic radius and diffusion coefficients. The influence of different macromolecular sizes of poly-L-SUL on the chiral separation of phenylthiohydantion (PTH)−amino acids and coumarinic derivatives, as test analytes, was elucidated by the use of micellar electrokinetic chromatography (MEKC). The size of polymeric surfactants as a prerequisite for chiral separation was demonstrated by comparing the separation properties of fractionated versus nonfractionated polymeric surfactants. Fractionated poly-L-SUL resulted in enhanced resolution and separation efficiency of the test analytes as compared to the case of the nonfractionated poly-L-SUL. This observation indicates that minimizing polydispersity of polymeric surfactants may be important for some chiral separation applications.

Introduction

Investigation of the potential utility of chiral surfactants as buffer additives in micellar electrokinetic chromatography (MEKC) is a recurring theme in the chiral separation literature. The Warner[1] and the Dobashi[2] groups reported the use of chiral polymeric surfactants for the separation of chiral compounds in 1994. Recently, a number of parameters that influence the chiral separation of analytes using polymeric surfactants as the pseudostationary phase have been investigated. These parameters include the effect of steric factors,[2,3] the number of chiral centers (dipeptides vs amino acids),[4] the amino acid order in the dipeptide surfactant headgroup,[5] and the depth of penetration of analytes into the micellar core on chiral recognition.[6,7]

A considerable interest in the use of polymeric surfactants arises because of several distinct advantages of polymeric surfactants over conventional micelles. Polymeric surfactants are covalently linked and, therefore, can be purified and used below the critical micelle concentration (cmc).[8,9] Covalently linked polymeric surfactants are polymerized above the cmc in order to ensure the presence of micelles during the polymerization process.[10] Conversely, polymerization above the cmc can result in a polydispersed distribution of macromolecular sizes.[11−13] Polydispersed polymeric surfactants consist of a nonuniform distribution of micelles with respect to relative molecular mass, constitution, or both.[14] The degree of polydispersity is larger for polymeric surfactants than for conventional micelles mostly because of possible incompatibility between the rate of micellization and the rate of polymerization.[15] Consequently, polymeric surfactants usually exhibit some degree of polydispersity with respect to size and shape.

Since the introduction of polymeric surfactants, limited studies have been performed to determine the effects of the structural characteristics of polydispersed surfactant solutions on chiral recognition.[16] A greater understanding of the effects of polymerization and the resulting polymeric

* Corresponding author. E-mail: iwarner@lsu.edu. Phone: 225-578-2829. Fax: 225-578-3971.

[†] Louisiana State University.

[‡] Carthage College.

(1) Wang, J.; Warner, I. M. *Anal. Chem.* **1994**, *66*, 3773−3776.
(2) Dobashi, A.; Hamada, M.; Dobashi, Y.; Yamaguchi, J. *Anal. Chem.* **1995**, *67*, 3011−3017.
(3) Thibodeaux, S. J.; Billiot, E.; Warner, I. M. *J. Chromatogr., A* **2002**, *966*, 179−186.
(4) Shamsi, S. A.; Macossay, J.; Warner, I. M. *Anal. Chem.* **1997**, *69*, 2980−2987.
(5) Billiot, E.; Macossay, J.; Thibodeaux, S. J.; Shahab, S.; Warner, I. M. *Anal. Chem.* **1998**, *70*, 1375−1381.
(6) Billiot, E.; Thibodeaux, S. J.; Shamsi, S.; Warner, I. M. *Anal. Chem.* **1999**, *71* (18), 4044−4049.
(7) Billiot, F. H.; Billiot, E.; Warner, I. M. *J. Chromatogr., A* **2002**, *950*, 233−239.
(8) Palmer, C. P. *Electrophoresis* **2002**, *23*, 3993−4004.
(9) Shamsi, S. A.; Palmer, C. P.; Warner, I. M. *Anal. Chem. A-Pages* **2001**, *73*, 140A−149A.
(10) Larrabee, C. E.; Sprague, E. D. *J. Polym. Sci., Polym. Lett. Ed.* **1979**, *17*, 749−51.
(11) Menger, F. M. *Acc. Chem. Res.* **1979**, *12*, 111−115.
(12) Ikeda, S. *J. Phys. Chem.* **1984**, *88*, 2144−2147.
(13) Mileva, E. *J. Colloid Interface Sci.* **2000**, *232*, 211−218.
(14) *IUPAC Compendium of Chemical Terminology*; Royal Society of Chemistry: Cambridge, U.K., **1996**; Vol. 68, pp 2287−2311.
(15) Yokozawa, T.; Suzuki, H. *J. Am. Chem. Soc.* **1999**, *121*, 11573−11574.
(16) Harrell, C. W.; McCarroll, M. E.; Morris, K. F.; Billiot, E. J.; Warner, I. M. *Langmuir* **2003**, *19*, 10684−10691.

10.1021/la036349s CCC: $27.50
Published on Web 07/02/2004

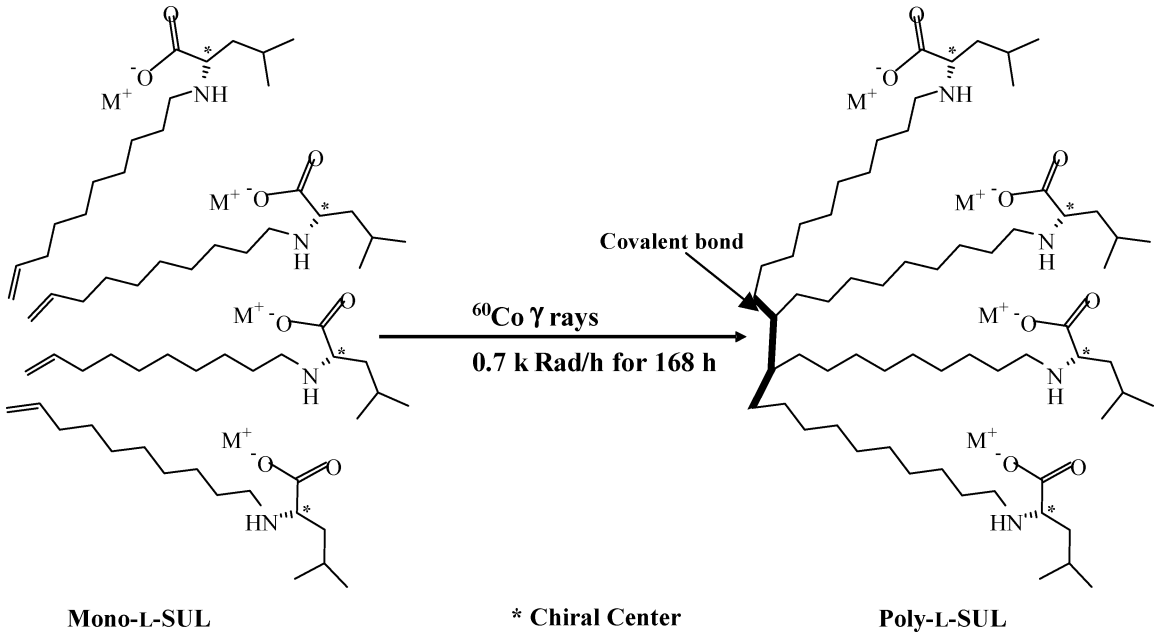

Figure 1. Chemical structure of *N*-undecenoyl-L-leucinate surfactant.

surfactant structures on chromatographic performance will facilitate the development of more effective new pseudostationary phases. To understand how different molecular weight distributions affect chiral separation in MEKC, polysodium undecenoyl-L-leucinate (poly-L-SUL) was fractionated into different molecular weights by the use of molecular weight cutoff (MWCO) centrifugal filters. Characterization of nonfractionated and fractionated polymeric surfactants was performed by use of three techniques: (1) pulsed field gradient nuclear magnetic resonance (PFG-NMR) was used to determine the hydrodynamic radii, (2) analytical ultracentrifugation (AUC) was used to determine the molecular weights, and (3) steady-state fluorescence was used to determine the polarity of the nonfractionated and fractionated polymeric surfactants. The effect of different sizes of polymeric surfactants on chiral separations was determined by employing nonfractionated and fractionated poly-L-SUL in MEKC. Phenylthiohydantion (PTH)−amino acids and coumarinic derivatives were used as test analytes. The separation parameters of these analytes from each of the fractionated and nonfractionated polymeric surfactants were evaluated and compared.

Experimental Section

Materials. The single amino acid L-leucine, the racemates of (±)-warfarin and (±)-coumachlor, and phenythiohydantoin (PTH)−DL-amino acids were purchased from Sigma (St. Louis, MO). *N*-hydroxysuccinimide, undecylenic acid, sodium bicarbonate, D_2O, pyrene, and dicyclohexylcarbodiimide (DCC) were obtained from Fluka (Milwaukee, WI) and were used without further purification. Ethyl acetate, methanol, cyclohexane, and tetrahydrofuran (HPLC grade) were obtained from Aldrich (Milwaukee, WI) and were used as received. Molecular weight cutoff (MWCO) centrifugal filters were purchased from Millipore (Billerica, MA).

Synthesis of Polymeric Surfactant. The polymeric surfactant was synthesized according to the procedure described by Wang et al.[17] Briefly, the amino acid, L-leucine, was reacted with the ester and sodium bicarbonate to form sodium undecenoyl-L-leucinate (L-SUL) and then polymerized (Figure 1). Polymerization was achieved by the use of γ-irradiation from a ^{60}Co source (model 484 R, from J. O. Shepherd, San Fernando, CA) of 0.7 krad/h for 168 h (total dose, 118 krad). Proton NMR was used to monitor the polymerization process. The disappearance of the vinyl proton signals at 6.0−5.0 ppm and the broadening of the low frequency peaks were taken to be indicators of a complete polymerization of the surfactant.

Centrifugation Filtration. Disposable, ultrafree 15 mL Millipore centrifugal filters of different sizes (5, 10, and 30K) were used to sieve (fractionate) poly-L-SUL. About 15 mL of polymeric surfactant aqueous solution (50 mM) was added into the desired centrifugal filter, capped tightly, and placed in a 50 mL centrifuge tube before centrifugation. Centrifugation was performed at a speed of 2000*g* for 6 h before replacing the filter. The desired surfactant fraction was collected at the bottom of the tube. The surfactant concentrate was filtered twice by the use of the desired MWCO filter in order to recover polymeric surfactants of a specific size range (for example, 5−10K).

Pulsed Field Gradient-NMR. Pulsed field gradient-NMR (PFG-NMR) experiments were performed by the use of a 300 MHz Bruker DPX spectrometer (Billerica, MA). The instrument's probe was equipped with an actively shielded *z*-gradient coil. A diffusion experiment with an aqueous β-cyclodextrin sample yielded a coil constant of 50.3 G/cm at 100% gradient strength.[18] The solutions for NMR analysis were prepared gravimetrically by dissolving 5−7 mg of polymeric surfactant in 1.00 mL of D_2O. Samples were placed in the NMR spectrometer and allowed to equilibrate at 25 °C for at least 60 min before data acquisition began. The diffusion coefficient (D) for each polymeric surfactant was measured with the bipolar pulse pair longitudinal encode−decode pulse sequence.[19] Fifteen free induction decays (FIDs) were collected for each sample with magnetic field gradient amplitudes (G values) ranging from 5.03 to 35.7 G/cm. Each individual FID contained 16K data points and was collected with a spectral width of 6000 Hz. The individual FIDs were then apodized with 5.0 Hz line broadening, Fourier transformed, and phased using the Bruker Xwinnmr 2.1 software package. The intensity (I) of the resulting spectra was calculated by the use of eq 1:

$$I = I_0 \exp\left[-D(\gamma G\delta)^2\left(\Delta - \frac{\delta}{3} - \frac{\tau}{2}\right)\right] \quad (1)$$

where I_0 is the resonance intensity with no magnetic field gradient, γ is the magnetogyric ratio, δ is the duration of the magnetic field gradient pulse, Δ is the diffusion time, and τ is

(17) Wang, J.; Warner, I. M. *Anal. Chem.* **1994**, *66*, 3773−3776.

(18) Uedaira, H.; Uedaira, H. *J. Phys. Chem.* **1970**, *74*, 2211−2214.

(19) Wu, D.; Chen, A.; Johnson, C. S., Jr. *J. Magn. Reson., Ser. B* **1995**, *115*, 260−264.

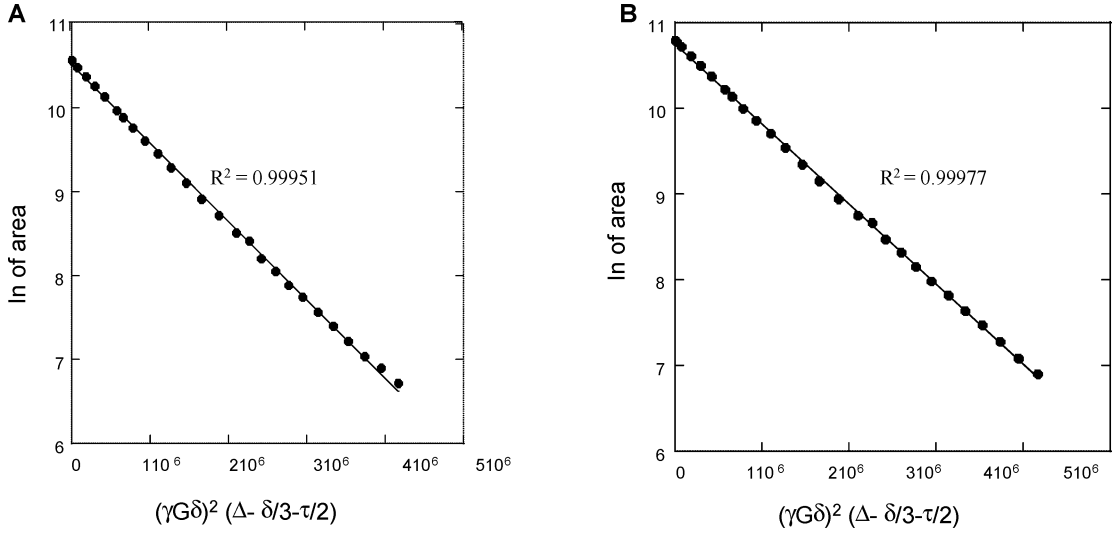

Figure 2. Echo intensity decay with magnetic field gradient strength for (A) nonfractionated poly-L-SUL and (B) fractionated above 30K poly-L-SUL.

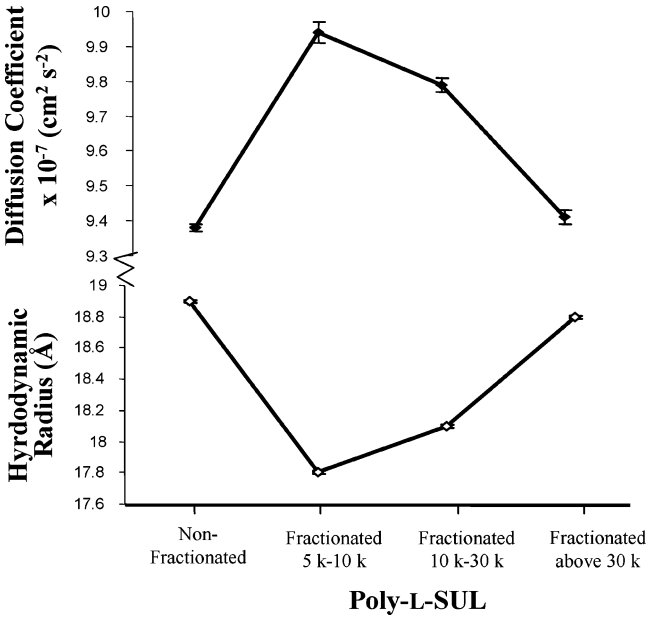

Figure 3. Plots of diffusion coefficients (upper plot) and hydrodynamic radii (lower plot) of nonfractionated and fractionated poly-L-SUL surfactants.

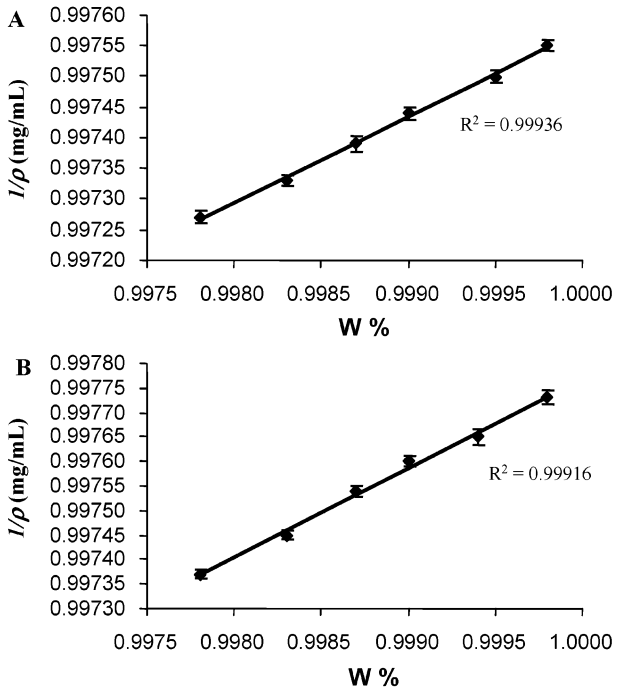

Figure 4. Plot of $1/\rho$ (mg/mL) as a function of W [(weight of solvent)/(weight of solvent + weight of solute)]. The representative samples are (A) nonfractionated poly-L-SUL and (B) fractionated above 30K poly-L-SUL. The reproducibility of points ($n = 4$) was ~4.61% relative standard deviation (RSD).

the short delay between the bipolar gradients. Throughout this study, δ, Δ, and τ had respective values of 4.0, 250.0, and 0.20 ms. For each of the 15 spectra in the resulting data set, the resonances in the region from 0.85 to 1.50 ppm were integrated and plots of the natural log of the peak integral versus the quantity $(\gamma G\delta)^2(\Delta - \delta/3 - \tau/2)$ were prepared. Linear regression analysis of the resulting graph provided the diffusion coefficient (D). The computed diffusion coefficients obtained from linear regression analysis data were then used to calculate the hydrodynamic radius (R_h) of each polymer via the Stokes−Einstein equation given by

$$D = \frac{k_B T}{6\pi\eta R_h} \qquad (2)$$

where k_B is Boltzmann's constant, T is the temperature in kelvins, and η is the solvent viscosity (1.232 cP for D_2O at 298 K).[20] The Stokes−Einstein equation assumes that the polymers adopt a spherical shape in solution. Linear regression analysis was used to extract the diffusion coefficients because the signal-to-noise ratio was very high in the methylene region of each spectrum. The R^2 values for all of the linear regression analyses were equal to or greater than 0.999.

Densitometry. A high-precision densitometer (model DMA58), purchased from Anton Paar USA (League City, TX), was used to perform density measurements. Air and water were used for calibration. The precision of the temperature-controlled system was better than ±0.005 °C.

Analytical Ultracentrifugation. Equilibrium sedimentation measurements for determining the molecular weight of the polymeric surfactant were performed by the use of an Optima XLA analytical ultracentrifuge instrument from Beckman Instruments, Inc. (Palo Alto, CA). The instrument has a high-intensity xenon flash light source and a grating monochromator with continuous scanning from 190 to 800 nm. The detection system was set to measure the absorbance at 220 nm. The flash

(20) Kellomaki, A. *Finn. Chem. Lett.* **1975**, *51*, 23−23.

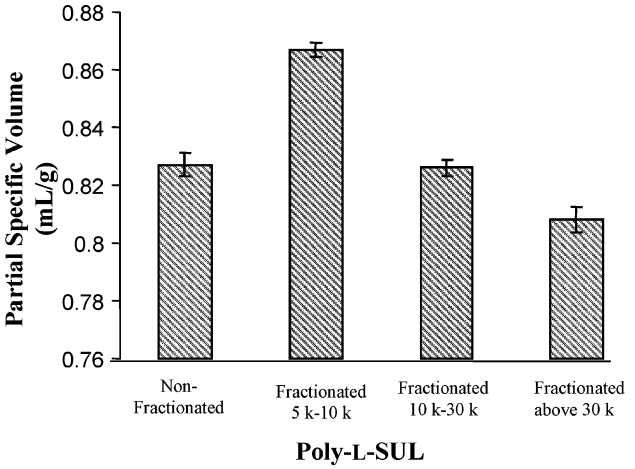

Figure 5. Plot of the partial specific volumes of poly-L-SUL surfactant fractions.

lamp illuminated only a selected sample during the scanning. A toroidally curved holographic diffraction grating was used to select the wavelength and to collimate the beam of light. Four sector cells were used, and data were acquired every 10 μm in replicates of 10. These data were digitized and displayed as a function of radial distance. The sample volumes were 100 μL, while the solvent volumes were 125 μL. The data were collected at a speed of 22 000 rpm. The temperature of the rotor was controlled thermoelectrically to within ±0.5 °C. All samples had a polymer concentration of 0.1 g/L. The absorbance versus the distance from the center of rotation to any position in the sample column was collected at 720 min intervals. Successive scans of the cell were compared graphically using the XL software to ensure that the samples reached equilibrium.

Fluorescence Measurements. Fluorescence measurements used to determine the polarity of the micelles were acquired at room temperature on a Spex FluoroMax-3 spectrophotometer (model FL3-22TAU3) from Jobin Yvon Inc. (Edison, NJ). The excitation and emission slits were maintained at 2 and 3 nm, respectively. A stock solution of pyrene (2×10^{-4} M) was prepared in cyclohexane. An appropriate aliquot of pyrene from the stock solution was transferred into a flask and dried under a gentle stream of nitrogen. Triply distilled deionized water was added to the flask and sonicated for 1 h to give a 2×10^{-8} M pyrene solution. Weighed amounts of nonfractionated and fractionated poly-L-SUL surfactants were dissolved in 2×10^{-8} M aqueous pyrene solution, resulting in a final concentration of 6 mM surfactant. A low concentration of pyrene reduces the probability of multiple probe molecules per micelle. It should be noted that the solubility limit of pyrene in water is 6×10^{-7} M.[21] The resulting pyrene-polymeric surfactant solution mixture was sonicated for 1 h and left to equilibrate overnight before the fluorescence measurements. The equilibrated solutions were excited at 335 nm and the emission intensities measured from 360 to 500 nm. The I_1/I_3 ratio was obtained at 373 (I_1) and 383 (I_3) nm wavelengths.

Capillary Electrophoresis. The MEKC experiments were conducted by the use of a 3DCE instrument (model G1600AX), from Agilent (Palo Alto, CA). A positive voltage of 30 kV was supplied throughout the experiment, with UV detection at 215 and 254 nm. The injection size for all analytes was 30 mbar for 3 s. A fused silica capillary (Polymicro Technologies, Phoenix, AZ) of a 60 cm effective length and 50 μm inside diameter (i.d.) was initially conditioned for 2 h with 1 M NaOH and then 30 min with 0.1 M NaOH at 30 °C. The capillary was finally rinsed for 10 min with deionized water and for 10 min with the buffer of interest prior to use. Fresh surfactant solutions were prepared daily, filtered through a 0.45 μm polypropylene filter, and degassed for at least 5 min prior to each experiment. The desired temperature of the capillary was maintained using the instrument's thermostating system. The MEKC experiments of PTH−amino acids and coumarinic derivatives were conducted at 15 °C.

Buffer and Sample Preparation for MEKC. All analyte stock solutions were prepared at a concentration of 10 mg/mL in methanol. An appropriate aliquot of each analyte was transferred to a sample vial and diluted with methanol. The final concentration of each analyte in the mixture was ~0.10−0.15 mg/mL. A buffer solution of 275 mM boric acid, 20 mM sodium phosphate, and 10 mM triethylamine was prepared in triply deionized water. Each fractionated poly-L-SUL surfactant as well as nonfractionated poly-L-SUL surfactant was dissolved in the buffer solution to give an equivalent monomer concentration of 50 mM (pH 7.00) for the separation of PTH−amino acids and coumarinic derivatives.

The retention factors (k' values), resolution factors (R_s values), and peak efficiencies (N values) were calculated using the following equations:[22]

$$k' = \frac{t_r - t_0}{t_0} \tag{3}$$

$$R_s = \frac{t_{r_2} - t_{r_1}}{w_1 + w_2} \tag{4}$$

$$N = 5.54\left(\frac{t_r}{w_{1/2}}\right)^2 \tag{5}$$

where t_0 and t_r are the respective migration times of the unretained species and the enantiomer and w is the peak width at the baseline of each enantiomer. The subscripts 1 and 2 in eq 4 refer to the first and last eluting enantiomer. The peak width at half-height is designated by $w_{1/2}$.

Results and Discussion

Figure 1 depicts the chemical structure of sodium undecenoyl-L-leucinate chiral surfactant monomers (mono-L-SUL). The L-SUL surfactant is composed of a C_{11} hydrocarbon chain with a polymerizable double bond and the amino acid leucine as a polar headgroup. Polymerization of SUL monomers above the cmc by the use of γ-irradiation from ^{60}Co resulted in poly-L-SUL (Figure 1).

PFG-NMR. Diffusion coefficients and hydrodynamic radii of poly-L-SUL surfactant fractions were determined by the use of PFG-NMR. Linear regression analysis of the PFG-NMR data provided the diffusion coefficient (D). Examination of the computed diffusion coefficient values revealed a lower diffusion coefficient for the nonfractionated poly-L-SUL as compared to the fractionated poly-L-SUL. An analysis of the plots in parts A (nonfractionated, $R^2 = 0.999\,51$) and B (fractionated above 30K, $R^2 = 0.999\,77$) of Figure 2 indicates both graphs are sufficiently linear. This observation is not surprising given ~70% of the total amount of the fractionated surfactant was obtained above 30K, while ~20% and ~10% were obtained for 10−30K and 5−10K, respectively. Therefore, much curvature is not observed for the nonfractionated sample as compared to the fractionated samples because the nonfractionated sample consisted of predominantly larger polymers. In addition, it is likely that the fractionated samples were rather monodispersed and contained a rather narrow distribution of molecular sizes after the centrifugal filtration process.

The plots in Figure 3 show the diffusion coefficients and the hydrodynamic radii of nonfractionated and fractionated poly-L-SUL. The diffusion coefficients of

(21) Wilhelm, M.; Zhao, C. L.; Wang, Y.; Xu, R.; Winnik, M. A. *Macromolecules* **1991**, *24*, 1033−1040.

(22) Terabe, S.; Otsuka, K.; Ichikawa, K.; Tsuchiya, A.; Ando, T. *Anal. Chem.* **1984**, *56*, 111−113.

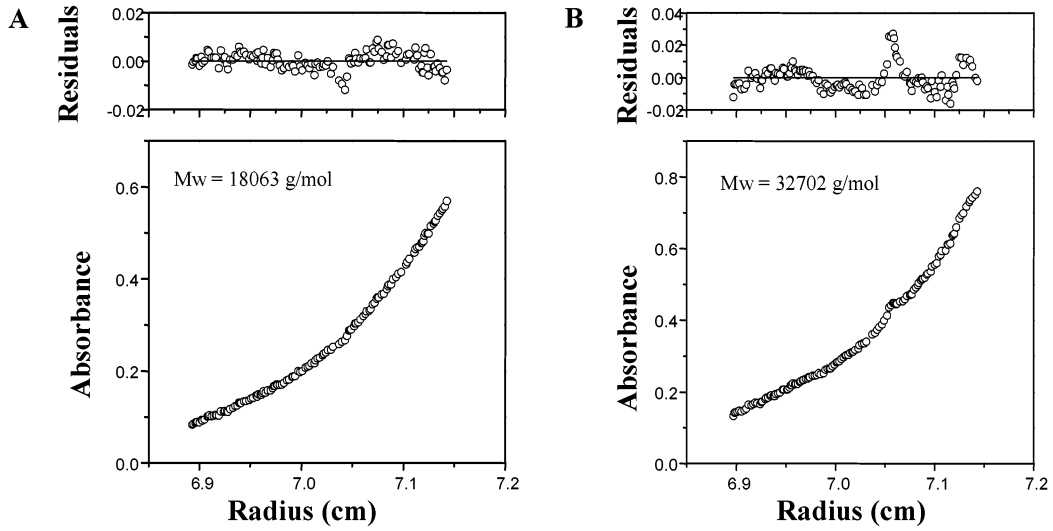

Figure 6. Plots and residuals of absorbance vs radius for two representative samples of poly-L-SUL, (A) nonfractionated poly-L-SUL and (B) fractionated above 30K poly-L-SUL. The residuals of the experimental data from the best fit line are shown in the top panel.

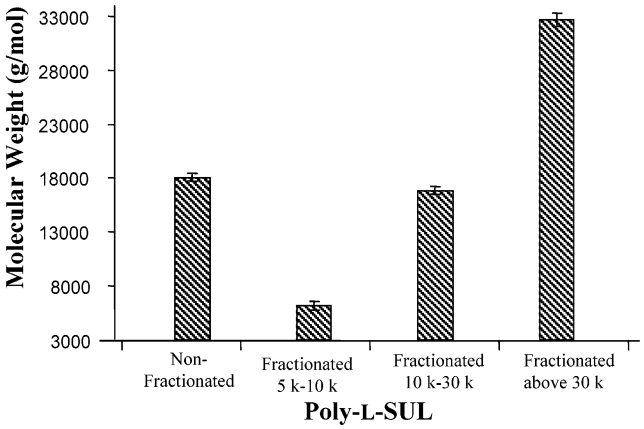

Figure 7. Plot of the molecular weights of nonfractionated and fractionated poly-L-SUL surfactants.

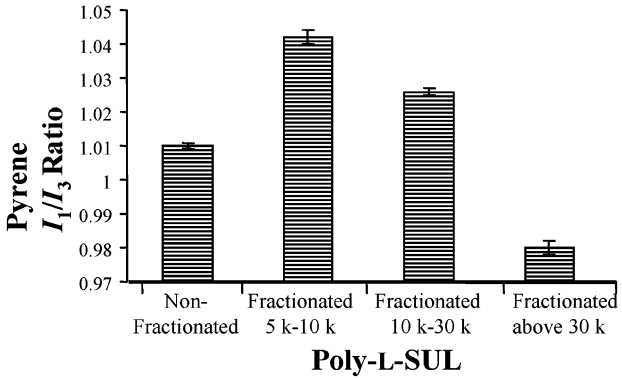

Figure 8. Pyrene I_1/I_3 polarity ratio of nonfractionated and fractionated poly-L-SUL.

fractionated poly-L-SUL surfactants decreased as the size of the MWCO filter increased. This observation implies that the diffusion of larger surfactant structures is slower than that of smaller surfactant structures. Typically, increasing the size of the MWCO filter resulted in a corresponding increase in the size of the polymeric surfactant, as evidenced by an increase in the hydrodynamic radii. It should be noted that the diffusion coefficients and hydrodynamic radii of both nonfractionated and fractionated poly-L-SUL (above 30K) are comparable (Figure 3). On the basis of the quantities of the fractionated surfactants obtained after centrifugal filtrations, it can be concluded that larger surfactant structures (above 30K) have a disproportionate effect on the diffusion properties of poly-L-SUL.

Determination of Partial Specific Volume and Molecular Weights by Analytical Ultracentrifugation. By definition, partial specific volume ($\bar{v}$) is the volumetric change when a small amount of dry solute (1 g) is dissolved in a large volume of the solvent. The $\bar{v}$ values were obtained by plotting the inverse of the density ($1/\rho$) of the aqueous polymer solutions as a function of the weight fraction (W). The inverse of the density is given by eq 6[23]

$$\frac{1}{\rho} = \bar{v} + W\frac{\partial(1/\rho)}{\partial W} \tag{6}$$

where ρ is the solution density and W is the solvent weight fraction. The partial specific volume of poly-L-SUL was obtained as the y-intercept of the $(1/\rho)$ versus W plot (Figure 4). The high-precision density measurements used to determine the $\bar{v}$ values resulted in linear plots (Figure 4). The partial specific volumes of poly-L-SUL fractions decreased as the size of the molecular weight cutoff filters increased (Figure 5). It is interesting to note that the $\bar{v}$ values for nonfractionated and 10−30K fractionated poly-L-SUL are similar despite the differences in the diffusion coefficients and hydrodynamic radii. This discrepancy can be attributed to the differences in the physical parameters measured by each technique. In addition, it is possible that a larger proportion of polymeric structures of a molecular weight of 30K or higher are contained in the nonfractionated and 10−30K fractionated poly-L-SUL. The observed variation in the $\bar{v}$ values with varying surfactant fractions suggests a possible change in the packing format in the polymeric surfactant and ease of interaction with the water molecules. It is noteworthy that surfactant molecular structure, hydration properties, and temperature contribute to the $\bar{v}$ value of a surfactant system.[24]

(23) Durchschlag, H. In *Thermodynamic data for biochemistry and biotechnology*; Hinz, H. J., Ed.; Springer-Verlag: New York, 1986.
(24) Steele, J. C. H., Jr.; Tanford, C.; Reynolds, J. A. *Methods Enzymol.* **1978**, *48*, 11−23.

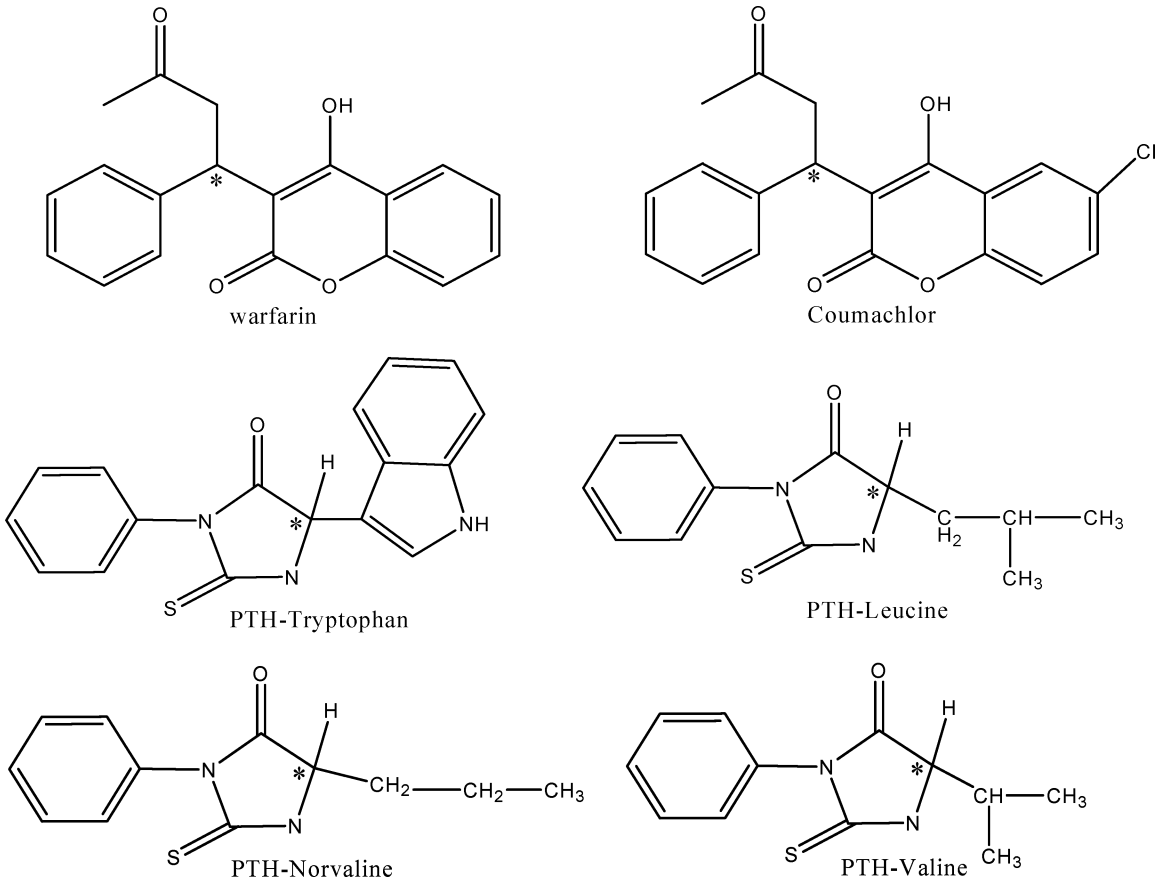

Figure 9. Chemical structures of the test analytes with chiral centers denoted by an asterisk.

The molecular weights of different fractions of poly-L-SUL surfactant were calculated from the $\bar{v}$ values and the sedimentation data obtained by the use of analytical ultracentrifugation (AUC).[25] It should be noted that the AUC equation used for the calculation of the molecular weights is suitable for monodispersed samples. For polydispersed samples, the equilibrium distribution plot deviates from linearity.[26] Consequently, the curvature of the equilibrium distribution data must be analyzed in order to obtain the average molecular weights at distance *r*.

Figure 6 illustrates the equilibrium distribution plot of two representative fractions at 25 °C. The residuals at the top of each plot indicate how well the data points correlate with the fitting function. The measured molecular weights of different fractions of poly-L-SUL are presented in Figure 7. Evidently, the average molecular weight of fractionated polymeric surfactants increased as the size of the MWCO filters increased in the order of 5−10K < 10−30K < above 30K. Notably, the average molecular weights of the nonfractionated and 10−30K fractionated poly-L-SUL are statistically the same. This observation is consistent with the results obtained for partial specific volume.

Polarity of Micelles. Fluorescence emissions of monomeric pyrene molecules solubilized in polymeric surfactants can be used to provide structural information on the micelles.[27−29] The monomer emission intensities between the first (373 nm) and the third (383 nm) vibronic peaks of the pyrene spectrum depend on the environmental polarity of the solubilized pyrene molecules.[30−32] The I_1/I_3 ratio is influenced by a number of factors including the aggregation number, core cavity, and core thickness of the micelle.[33] Therefore, it is possible to elucidate the location of pyrene molecules as a function of the size of the micelle from the I_1/I_3 ratio.

In the present study (Figure 8), the I_1/I_3 ratio decreased as the size of the fractionated polymeric surfactant increased in the order of 5−10K > 10−30K > above 30K. The shift of the I_1/I_3 ratio from a higher value (1.045) for the 5−10K fractionated poly-L-SUL to a smaller value (0.98) for the poly-L-SUL fractionated above 30K MWCO filter indicated that more of the solubilized pyrene molecules resided in a hydrophobic environment. If pyrene molecules were distributed only in the palisade layer, then the I_1/I_3 ratio would not change when the size of the polymeric surfactant increased. The hydrophobic core increases as the size of the polymeric surfactant increases. Therefore, larger surfactant structures contribute to a remarkable decrease in the I_1/I_3 ratio, as indicated by the trend in polarity values (5−10K > 10−30K > above 30K) in Figure 8. It can be concluded that larger polymeric surfactant structures have very little space between the surfactant molecules and contain a large hydrophobic

(25) Fujita, H. In *Foundations of Ultracentrifugal Analysis*; Elving, P. J., Wineforder, J. D., Eds.; Wiley and Sons: New York, 1975.
(26) Correia, J. J.; Shire, S.; Yphantis, D. A.; Schuster, T. M. *Biochemistry* **1985**, *24*, 3292−3297.
(27) Narayanan, R.; Paul, R.; Balaram, P. *Biochim. Biophys. Acta* **1980**, *597*, 70−82.
(28) Valero, M.; Del Arco-Gomez, A.; Rodriguez, L. J. *J. Inclusion Phenom. Macrocyclic Chem.* **2002**, *42*, 121−130.
(29) Almgre, M.; Loefroth, J. E.; Rydholm, R. *Chem. Phys. Lett.* **1979**, *63*, 265−268.
(30) Nakijima, A. *Bull. Chem. Soc. Jpn.* **1971**, *44*, 3272−3277.
(31) Gratzel, M.; Kalyanasundaram, K.; Thomas, J. K. *J. Am. Chem. Soc.* **1974**, *96*, 7869−7874.
(32) Kalyanasundaram, K.; Thomas, J. K. *J. Am. Chem. Soc.* **1977**, *99*, 2039−2044.
(33) Turro, N. J.; Kuo, P.-L. *J. Phys. Chem.* **1986**, *90*, 4205−4209.

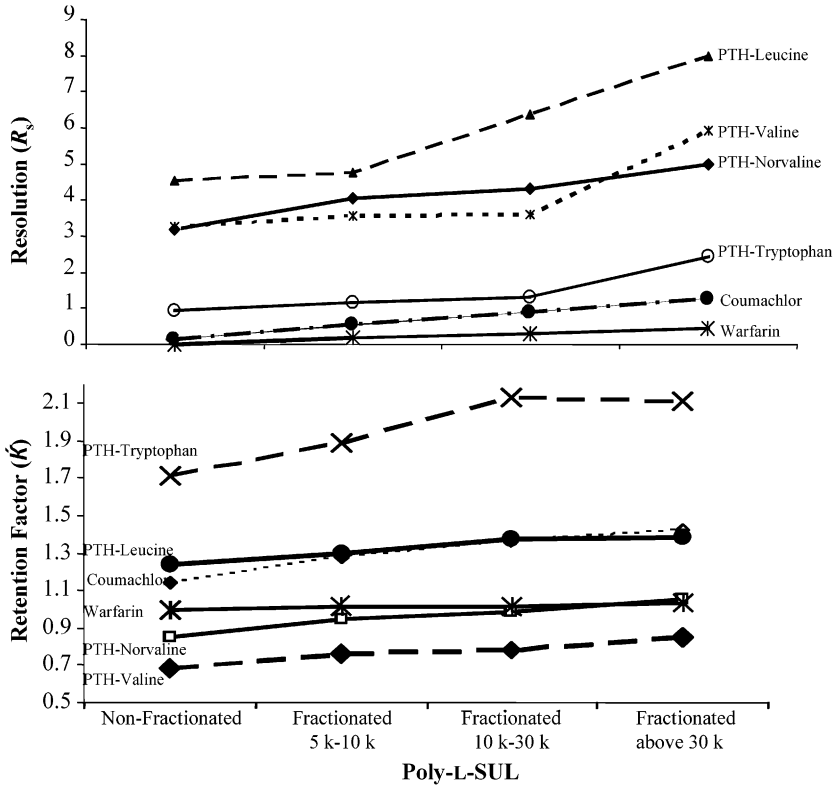

Figure 10. Effect of polydispersity on the resolution (upper plot) and retention (lower plot) of the test analytes in MEKC. Conditions for PTH−amino acid derivatives: +30 kV; 275 mM boric acid; 20 mM sodium phosphate; 10 mM triethylamine; pH 7.0; temperature, 15 °C; 50 mM (equivalent monomer concentration) poly-L-SUL; pressure injection, 30 mbar for 3 s of 0.10 mg/mL sample. Conditions for coumarinic derivatives: same as those in part a except a 0.15 mg/mL sample was used instead. The reproducibility of points ($n = 3$) was ~4.01% RSD for R_s and ~0.82% RSD for k'.

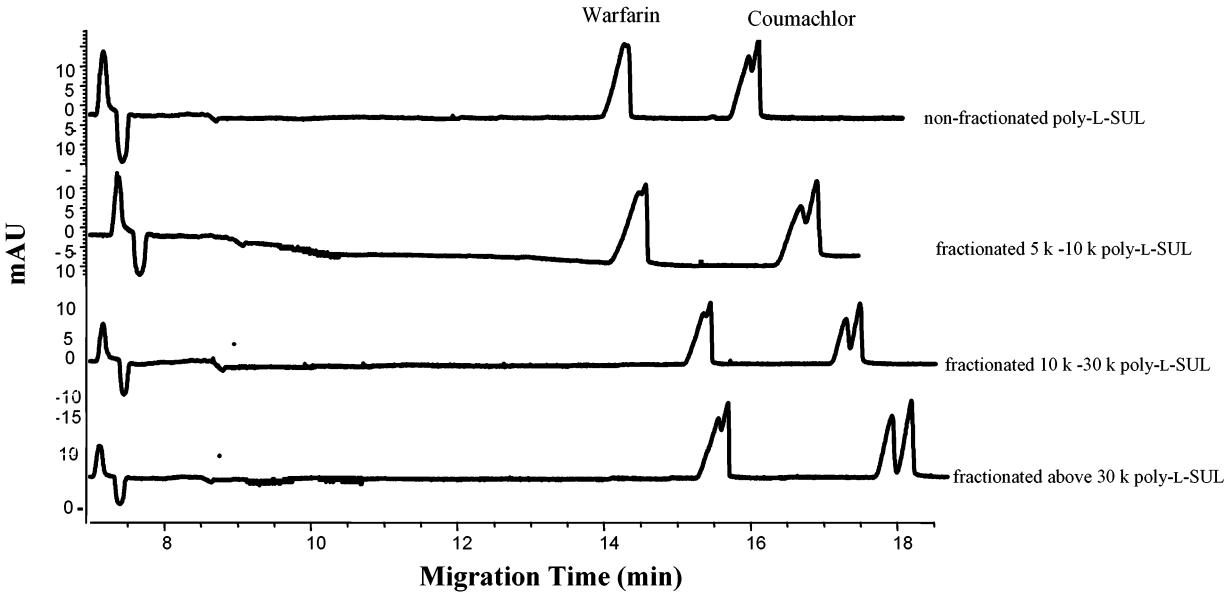

Figure 11. Effect of polydispersity on the chiral separation of (±)-warfarin and (±)-coumachlor. MEKC conditions: same as those in Figure 10.

domain; thus, they are poorly hydrated. Conversely, smaller polymeric surfactants allow more water molecules in the macromolecular structure. Consequently, larger sizes of poly-L-SUL provide smaller values of the I_1/I_3 ratio because of the larger hydrophobic domain of the polymeric surfactant. However, the nonfractionated poly-L-SUL I_1/I_3 ratio is comparable to that of the 10−30K fractionated poly-L-SUL. This observation can be explained by considering the presence of a large percentage (≈70%) of polymeric surfactant of a molecular weight of 30K or higher in the nonfractionated poly-L-SUL.

MEKC Studies. The polydispersity of polymeric surfactants employed in MEKC adversely affects the electrokinetic separations of the analytes.[34] This is because wide ranges of micelle migration velocities result in band broadening. To understand how different sizes of polymeric

(34) Palmer, C. P.; Terabe, S. *Anal. Chem.* **1997**, *69*, 1852−1860.

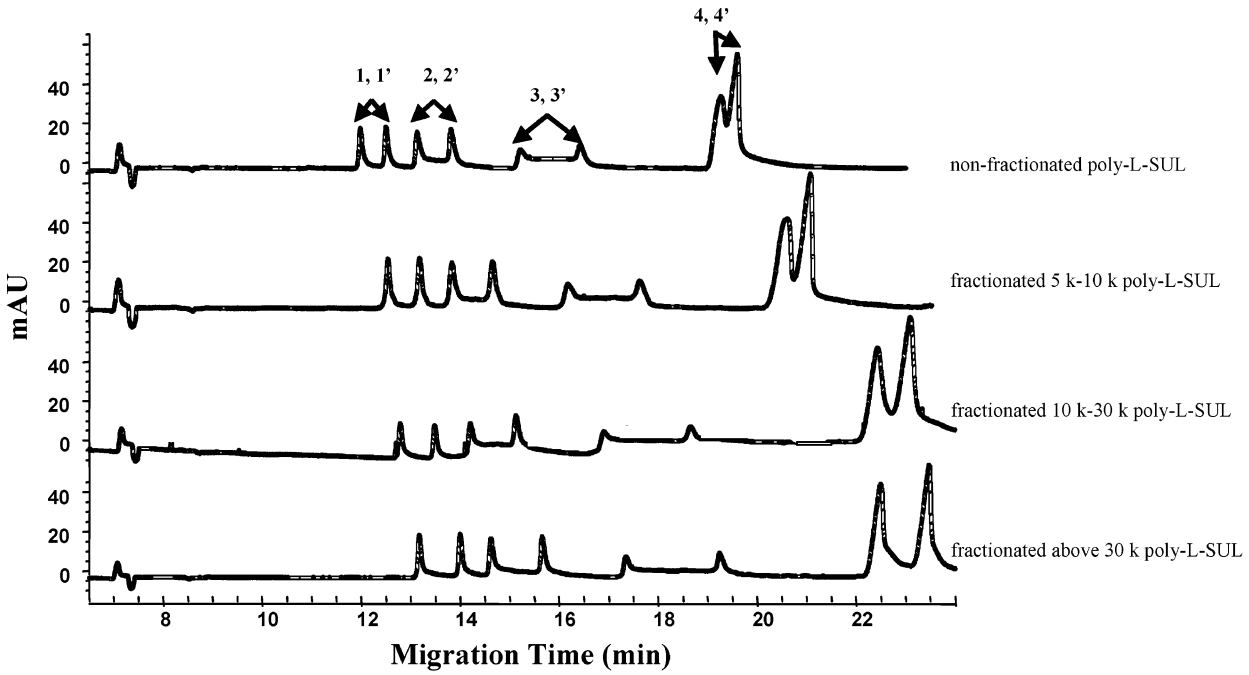

Figure 12. Effect of polydispersity on the chiral separation of PTH−amino acid derivatives (1,1′-PTH−valine, 2,2′-PTH−norvaline, 3,3′-PTH−leucine, and 4,4′-PTH−tryptophan). MEKC conditions: same as those in Figure 10.

surfactants affect electrokinetic separations of analytes in MEKC, we compared the enatiomeric separation of coumarinic derivatives and PTH−DL-amino acids (see Figure 9 for structures) in nonfractionated and fractionated samples of poly-L-SUL. These analytes were chosen because they are hydrophobic and neutral under the buffer conditions used. In addition, the hydrophocibity of PTH−amino acids depends on the structure of the amino acid residue in the order of PTH−valine < PTH−norvaline < PTH−leucine < PTH−tryptophan.

The chiral center of poly-L-SUL (Figure 1) is the active site for the enantiomeric resolution of analytes in MEKC. The enantiomeric resolution is based on interactions between the enantiomer, the chiral polymeric surfactant, and the buffer. The *iso*butyl groups of poly-L-SUL enhance the interactions between the chiral center of the enantiomeric compound and the surfactant's polar head by imparting a stereospecific interaction. These *iso*butyl residues control the degree of interaction between the enantiomer, the polar groups, and the hydrophobic groups around the chiral center. Consequently, the enantiomer interacts with poly-L-SUL, forming diastereomeric complexes that have different formation constants. Polymeric surfactants fractionated to different sizes introduce unique hydrophobic interactions necessary for the chiral separation. Hydrophobic interaction plays a major role in the interaction between the solute and the pseudostationary phase.[35] In addition, different sizes of polymeric surfactants in the MEKC buffer have several consequences, the most important being a change in the partitioning of the analyte between the pseudostationary phase and the buffer phase resulting in different migration times for the analyte.

During separation, analytes differentially interact between the micellar phase and the bulk aqueous phase. Therefore, the observed migration times depend on the extent to which analytes partition between the surfactant and the aqueous phases. Hydrophobic analytes tend to be strongly associated with the hydrophobic domain of the surfactant and hence travel slower and elute later than the hydrophilic analytes (Figure 10). Consequently, hydrophobic characteristics of both the analyte and the surfactant largely determine the retention of the species in surfactant solution during separation. A general increase in the retention factors for all the test analytes was observed as the size of the fractionated poly-L-SUL was increased (Figure 10). As a result, an improvement in resolution was observed at the expense of analysis time for most test analytes (Figure 10). The elution time of the electro-osmotic flow (EOF) in these systems is depicted in the electropherograms in Figures 11 and 12 at ~7.5 min. Methanol was used as the EOF marker in these systems because it is not associated with the polymeric surfactant. It is noteworthy that larger surfactant structures, as reflected by their large molecular weights, slower diffusions, and larger hydrodynamic radii, migrate very slowly in the capillary. Consequently, factors such as the size and hydrophobicity of both the surfactant and the analyte affect the elution of the analytes in CE.

The effect of the polydispersity of poly-L-SUL on separation in MEKC was determined by comparing the separation efficiencies (*N* values) of fractionated and nonfractionated surfactant (eq 5). Typically, dispersion with the use of either monomeric or polymeric surfactants has been ascribed to experimental parameters[36−39] and surfactant properties.[38,40,41] Dispersion associated with surfactant properties are polydispersity,[38] slow kinetic processes between analytes and surfactants,[40] and mass transfer in the intermicellar phase.[41] A comparison of the separation efficiencies of the test analytes is demon-

(35) Alison, E. B.; Graham, S. C. *J. Chromatogr., A* **1995**, *716*, 49−55.

(36) Balchunas, A. T.; Sepaniak, M. J. *Anal. Chem.* **1988**, *60*, 617−621.

(37) Vindevogel, J.; Sandra, P. *Introduction to Micellar Electrokinetic Chromatography*; Huthig Bush: Heidelberg, Germany, **1992**.

(38) Terabe, S.; Otsuka, K.; Ando, T. *Anal. Chem.* **1989**, *61*, 251−260.

(39) Schure, M. R.; Lenhoff, A. M. *Anal. Chem.* **1993**, *65*, 3024−3037.

(40) Almgren, M.; Grieser, F.; Thomas, J. K. *J. Am. Chem. Soc.* **1979**, *101*, 279−291.

(41) Sepaniak, M. J.; Cole, R. O. *Anal. Chem.* **1987**, *59*, 472−476.

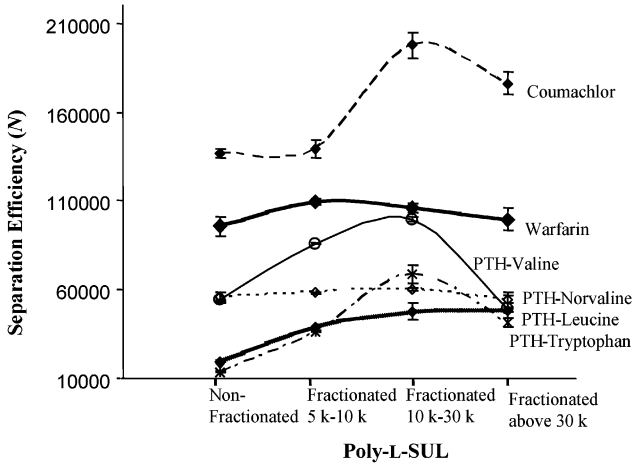

Figure 13. Plots of the peak efficiencies of the test analytes vs different poly-L-SUL surfactant fractions.

strated in Figure 13. It is interesting to note that all analytes except warfarin and PTH−valine depicted larger plate numbers in fractionated poly-L-SUL as compared to nonfractionated surfactant. A maximum peak efficiency of all the test analytes except warfarin was observed for 10−30K fractionated poly-L-SUL. It can be argued that the observed enhanced resolution obtained when fractionated surfactants are used is due to increases of partitioning, separation efficiency, selectivity, and a reduction in polydispersity. A decrease in *N* for surfactant fractionated above 30K is attributed to longitudinal diffusion due to longer retention times of the analytes.

Conclusions. In the study reported here, the influence of polydispersity on the separation properties of poly-L-SUL was examined. From the PFG-NMR, AUC, polarity, and MEKC data, it is noted that poly-L-SUL with a molecular weight between 10 and 30K and above 30K provides a more remarkable effect on chiral separation as compared to the case of nonfractionated poly-L-SUL. While the fluorescence results showed a decreasing polarity with an increasing size of fractionated polymeric surfactant, the PFG-NMR and AUC results depicted an increase in the hydrodynamic radii and molecular weight, respectively. In all characterization results, it was noted that the properties of nonfractionated poly-L-SUL closely match those of polymeric surfactant fractionated between 10 and 30K and above 30K. This observation is intuitive and implies that poly-L-SUL is largely comprised of large molecular weight structures. Examination of the MEKC data suggests enhanced separation of chiral compounds is both analyte and polymeric size dependent. For all the test analytes except warfarin, enantiomeric separation increased with increasing size of the polymeric surfactant. In addition, the narrowing of polydispersity by centrifugation filtration minimized band broadening, as demonstrated by increased separation efficiencies. The resulting enhanced resolution of the test analytes in MEKC is therefore attributed to a reduction of the dispersion effect due to the polydspersed distribution of poly-L-SUL surfactant structures and improved partitioning of analytes into the pseudostationary phase.

Acknowledgment. I.M.W. is grateful to the National Institutes of Health (GM 39844-12), National Science Foundation (CHE-0091726), and the Philip West Endowment for financial support of this investigation.

LA036349S